# Experimental and Computational Characterization of the Transition State for C–X Bimetallic Oxidative Addition at a Cu–Fe Reaction Center

**ARTICLE** *in* ORGANOMETALLICS · JULY 2015

Impact Factor: 4.13 · DOI: 10.1021/acs.organomet.5b00476



**4 AUTHORS**, INCLUDING:

Malkanthi Karunananda
University of Illinois at Chicago
**4** PUBLICATIONS **10** CITATIONS

SEE PROFILE

Neal Mankad
University of Illinois at Chicago
**50** PUBLICATIONS **1,259** CITATIONS

SEE PROFILE

ORGANOMETALLICS

Article

pubs.acs.org/Organometallics

# Experimental and Computational Characterization of the Transition State for C−X Bimetallic Oxidative Addition at a Cu−Fe Reaction Center

Malkanthi K. Karunananda,[†] Sean R. Parmelee,[†] Greyson W. Waldhart, and Neal P. Mankad*

Department of Chemistry, University of Illinois at Chicago, 845 W. Taylor Street, Chicago, Illinois 60607, United States

Supporting Information

**ABSTRACT:** The heterobimetallic complex (IPr)Cu-Fp (IPr = *N*,*N*′-bis(2,6-diisopropylimidazol-2-ylidene, Fp = $FeCp(CO)_2$) was identified previously as a nonprecious metal catalyst for C−H borylation. To better understand the nature of the bimetallic reaction pathways operative in this system, we have conducted a thorough mechanistic study of alkyl halide activation by the Cu−Fe heterobimetallic reaction center. Use of cyclopropylmethyl halide substrates as radical clocks established that alkyl halide activation occurs by a two-electron mechanism for alkyl bromides and chlorides but not iodides. Eyring analysis of the activation of benzyl chloride allowed for experimental determination of activation parameters, including a large and negative entropy of activation ($\Delta S^{\ddagger}$ = −36 eu). A Hammett study with *para*-substituted benzyl chlorides revealed a reaction constant of $\rho$ = 1.6, indicating accumulation of negative charge in the transition state on the alkyl halide carbon. The Ru analogue, (IPr)Cu-Rp (Rp = $RuCp(CO)_2$), was found to react approximately 17−25 times more slowly with selected benzyl chlorides than (IPr)Cu-Fp, indicating that the relative nucleophilicities of the free metal carbonyl anions are predictive of the relative reactivities of their heterobimetallic counterparts. Synthesis and characterization of the new Ag and Au analogues, (IPr)Ag-Fp and (IPr)Au-Fp, are reported along with the observation that these more covalent congeners are significantly less reactive toward alkyl halides. DFT calculations were used to model a transition state for the Cu−Fe reaction, which was identified as stereoinvertive at the alkyl halide carbon. NBO calculations indicate crucial roles played by the CO ligands within the Fp group: they both act as redox noninnocent ligands and also provide structural templating to stabilize the transition state as the metal−metal bond breaks.

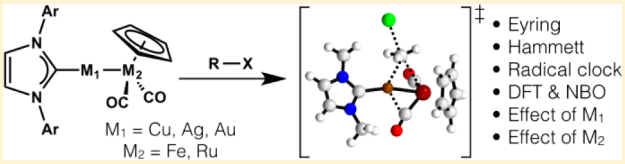


## INTRODUCTION

The mechanisms of oxidative addition (OA) and reductive elimination (RE) at single metal sites have been subject to intense study, in part due to their versatility in a wide range of important catalytic transformations. Analogous reactions of higher nuclearity, for example bimetallic oxidative addition (BOA) and bimetallic reductive elimination (BRE) at binuclear sites, are comparatively underexplored mechanistically, as well as for catalytic applications.[1−4] While many studies on BOA and BRE mechanisms have been reported with precious metals,[5−48] which are also typically capable of conducting single-site OA/RE chemistry, BOA and BRE pathways become particularly intriguing when they feature earth-abundant first-row transition metals not usually associated with single-site OA/RE independently.[49] Mechanistic studies on such bimetallic pathways are more limited in number.[50−62]

Our group recently reported that the heterobimetallic complex (IPr)Cu-Fp (IPr = *N*,*N*′-bis(2,6-diisopropylphenyl)-imidazol-2-ylidene, Fp = $FeCp(CO)_2$) is a catalyst for the C−H borylation of arenes,[63] a reaction more typically conducted using single-site OA/RE cycling by Ir catalysts.[64] The proposed mechanism for this reaction involves B−H BOA and H−H BRE processes that are unavailable to the Cu-only and Fe-only fragments that compose the heterobimetallic catalyst.[65] However, these specific BOA and BRE processes have proven difficult for us to probe experimentally with regard to mechanistic detail, and so we have been restricted to a predominantly computational mechanistic study.[66] Motivated to better understand the nature of the bimetallic reaction pathways available to (IPr)Cu-Fp through experimental data, we have chosen to examine carefully the mechanism of carbon−halogen activation by this heterobimetallic species.[67] We previously reported a spectroscopic study that elucidated the redistribution of electron density during methyl iodide BOA by (IPr)Cu-Fp and related complexes.[68] In the current report, we describe a combined experimental/computational study of the mechanism for alkyl halide BOA by (IPr)Cu-Fp and provide insight into its proposed bimetallic transition state.

## RESULTS AND DISCUSSION

**Single-Electron versus Two-Electron Pathways.** We previously reported that the complexes (IPr)Cu-Fp and (IMes)Cu-Fp (IMes = *N*,*N*′-bis(2,4,6-trimethylphenyl)-imidazol-2-ylidene) activate methyl iodide slowly at room temperature, producing the corresponding (NHC)Cu-I and Fp-$CH_3$ products cleanly (NHC = N-heterocyclic carbene).[67]

**Received:** June 5, 2015
**Published:** July 21, 2015





DOI: 10.1021/acs.organomet.5b00476
*Organometallics* 2015, 34, 3857−3864

However, no other alkyl halide substrates were tested. Subsequent spectroscopic and computational analyses of the starting point and end point of this methyl iodide reaction revealed that the Cu and Fe centers participate to a surprisingly limited extent in the redox changes in the formally BOA process, whereas the redox noninnocent CO ligands within the Fp group bear a large portion of the redox changes.[68] However, no information about the pathway for alkyl halide activation was probed in that study. Before embarking on reaction kinetics analysis, we first sought to establish that the BOA process occurs by a two-electron pathway rather than by a pathway involving radical intermediates. To do this, we examined the behavior of cyclopropylmethyl halide substrates (Table 1).

**Table 1. Reaction Profiles of (IPr)Cu-Fp and Na[Fp] with Radical Clock Substrates**[a]

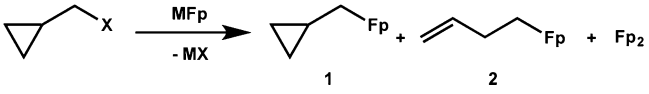


| M | X | 1 | 2 | $Fp_2$ |
|---|---|---|---|---|
| (IPr)Cu | Br | >97% | 0% | 0% |
| (IPr)Cu | I | 0% | 18% | 52% |
| Na | Br | >97% | <3% | 0% |
| Na | I | 52% | 30% | 19% |

[a]Conditions: THF, room temperature, overnight (~18 h).

The reaction between (IPr)Cu-Fp and cyclopropylmethyl bromide in THF at room temperature produced (IPr)Cu-Br and the Fp-R species **1**, with no evidence for the ring-opened form **2**. This observation indicates that the activation of alkyl bromide substrates by (IPr)Cu-Fp does not involve any radical intermediates with lifetimes of $10^{-8}$ s or more[69] and, likely, represents a *bona fide* two-electron reaction (or one with two single electron transfer events in rapid succession). On the other hand, the reaction between (IPr)Cu-Fp and cyclopropylmethyl iodide produced (IPr)Cu-I along with predominantly $Fp_2$, a signature of $Fp^{\bullet}$ formation, as the major Fe-containing product (52%). Minor products included a small (18%) amount of ring-opened **2**, a signature of the cyclopropylmethyl radical, as well as a complicated mixture of unidentified species. No evidence of **1** was found. These observations indicate that the activation of alkyl iodide substrates by (IPr)Cu-Fp involves radical intermediates, presumably formed by initial reduction of the alkyl iodide substrate by the electron-rich Fe center. While alkyl chlorides were not probed in this manner, we assume that they behave like alkyl bromides in their reactions with (IPr)Cu-Fp.

It is useful to compare these results with those for the bare $[Fp]^-$ anion, which also is known to activate alkyl halide substrates readily by an $S_N2$ mechanism.[70] Krusic et al. reported in 1977 that the reaction of Na[Fp] with cyclopropylmethyl bromide in THF at 0 °C produces a >97:<3 mixture of **1** and **2**, while the same reaction with cyclopropylmethyl iodide produces a 70:30 mixture of **1** and **2**.[71] In order to compare the chemistry of Na[Fp] directly with the chemistry of (IPr)Cu-Fp, and because the reactivity of (IPr)Cu-Fp at 0 °C is quite sluggish, we chose to repeat these seminal Na[Fp] experiments at room temperature (Table 1). In our hands, the reaction between Na[Fp] and cyclopropylmethyl bromide in THF at room temperature produced a >97:<3 mixture of **1** and **2**. The same reaction with cyclopropylmethyl iodide produced **1** (52%), **2** (30%), and $Fp_2$ (19%). Clearly, while both Na[Fp] and (IPr)Cu-Fp activate alkyl iodides using single-electron pathways, these pathways are distinct. This observation is important because it indicates that, in general, it is unlikely that the reactivity of (IPr)Cu-Fp proceeds through unmasking of the bare $[Fp]^-$ anion, but rather it occurs through distinct bimetallic pathways. Further discussion of this divergence will be included below.

**Reaction Kinetics.** Having established that alkyl bromide and chloride substrates participate in two-electron reaction pathways, we proceeded to analyze representative reaction kinetics using benzyl chlorides as substrates. Using the method of initial rates, a pseudo-first-order rate constant of $2.3(2) \times 10^{-5}$ $s^{-1}$ was measured for the reaction in toluene-$d_8$ at 298 K between (IPr)Cu-Fp and benzyl chloride, which yielded (IPr)Cu-Cl and $PhCH_2Fp$ as products. An Eyring analysis over the temperature range 273−373 K gave a linear plot (Figure 1), indicating activation parameters of $\Delta H^{\ddagger}$ = 13(2) kcal/mol and $\Delta S^{\ddagger}$ = −36(7) eu. The resulting $\Delta G^{\ddagger}$ = 24(3) kcal/mol calculated at 298 K is consistent with the qualitative observation that the reaction between (IPr)Cu-Fp and benzyl chloride is relatively sluggish at room temperature. The large and negative $\Delta S^{\ddagger}$ value is consistent with a highly organized transition state, as indicated by computational studies discussed below.

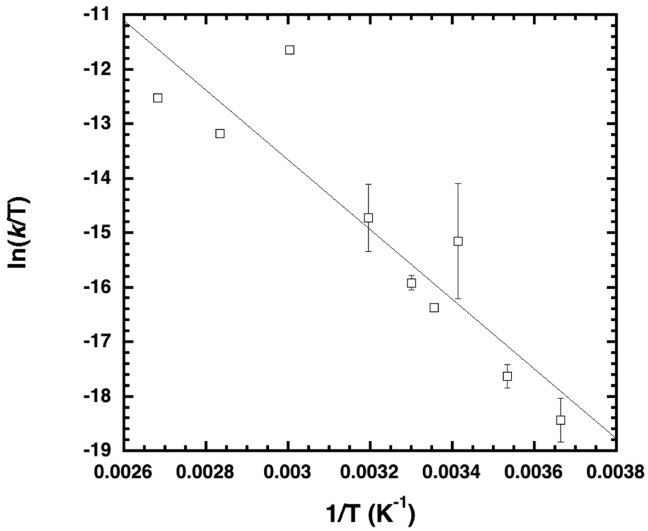


**Figure 1.** Eyring plot for the reaction between (IPr)Cu-Fp and benzyl chloride in toluene-$d_8$ from 273 to 373 K ($R^2$ = 0.821). Each data point results from a pseudo-first-order rate constant measured by the method of initial rates.

A Hammett analysis also was conducted at 298 K using *para*-substituted benzyl chloride substrates with various electron-donating (OMe, Me) and -withdrawing (Cl, $CO_2Me$, $CF_3$, CN) substituents. A linear free energy correlation emerged (Figure 2), indicating a reaction constant of $\rho$ = 1.6(2) when using standard $\sigma_{para}$ substitutent values. This reaction constant indicates that the reaction between (IPr)Cu-Fp and *para*-substituted benzyl chlorides is moderately accelerated by electron-withdrawing groups, consistent with a buildup of negative charge on the carbon atom of the C−X bond being activated.

Lastly, no experimentally determined Eyring activation parameters or Hammett reaction constants are available for


DOI: 10.1021/acs.organomet.5b00476
*Organometallics* 2015, 34, 3857−3864

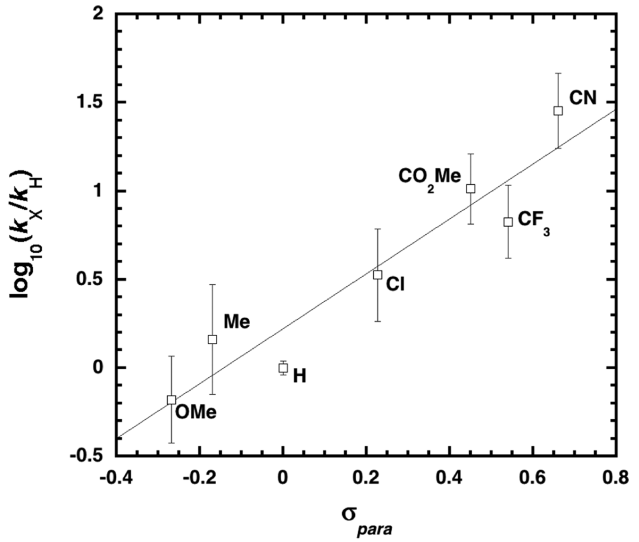


**Figure 2.** Hammett plot from reactions between (IPr)Cu-Fp and *para*-substituted benzyl chlorides in toluene-$d_8$ at 298 K (*para* substituents as indicated for each data point, $\rho$ = 1.6(2), $R^2$ = 0.905). Each data point results from a pseudo-first-order rate constant measured by the method of initial rates.

reactions between $[Fp]^-$ and alkyl halides for comparison. This absence is due in large part to the rapid rates of these reactions, precluding accurate rate constant measurements. Nonetheless, we note that these Fe-only reactions with alkyl chlorides and bromides are thought to occur by an $S_N2$ pathway due to the results of Krusic et al.'s radical clock experiments[71] as well as Whitesides's determination of stereochemical course.[72,73] This $S_N2$ reaction, with $[Fp]^-$ as the nucleophile and an alkyl halide as the electrophile, would also be expected to exhibit a large and negative $\Delta S^{\ddagger}$ as well as a reaction constant of $\rho > 1$. The Whitesides stereochemical probe did not react with either (IPr)Cu-Fp or (IMes)Cu-Fp, even after long reaction times or under forcing conditions. While this prevented us from experimentally determining the stereochemical course of alkyl halide activation by the (NHC)Cu-Fp complexes, it nonetheless further indicates that the (NHC)Cu-Fp complexes are not simply masked sources of $[Fp]^-$ but rather react by distinct bimetallic pathways. Nonetheless, from the perspective of the alkyl halide electrophile, the reaction resembles an $S_N2$ displacement, as indicated by both Eyring analysis and Hammett correlation.

**Effects of Metal Substitutions.** The $[Fp]^-$ anion is one of many metal carbonyl anions whose relative rates of nucleophilic reaction are well established.[74] We are tempted to use these reported values as predictors for the relative reactivity of different (NHC)Cu-[M] complexes toward electrophilic substrates ([M] = metal carbonyl anion), but this approach has not been validated experimentally. As a test case, we sought to examine the relative reactivity of (IPr)Cu-Fp versus (IPr)Cu-Rp (Rp = $RuCp(CO)_2$). Specifically, $[Fp]^-$ is known to be ~9 times more nucleophilic than $[Rp]^-$.[74] Does this mean (IPr)Cu-Fp is ~9 times more reactive toward alkyl halides than (IPr)Cu-Rp?

No reaction was observed between (IPr)Cu-Rp and benzyl chloride at room temperature over several days. However, benzyl chloride substrates with strong electron-withdrawing groups in the *para* position did react rapidly enough to obtain pseudo-first-order rate constants (Table 2). When comparing

**Table 2. Pseudo-First-Order Rate Constants for Benzyl Chloride Activation**[a]

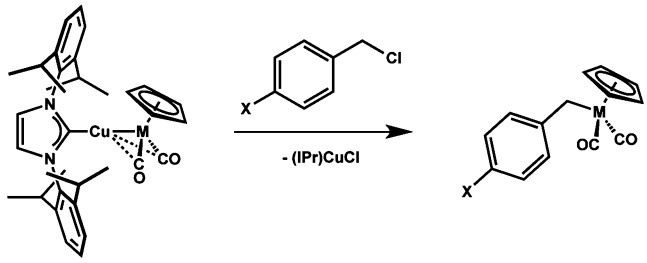


| X | M = Fe | M = Ru |
|---|---|---|
| $CF_3$ | 1.6(7) × $10^{-4}$ $s^{-1}$ | 7(2) × $10^{-6}$ $s^{-1}$ |
| CN | 6(3) × $10^{-4}$ $s^{-1}$ | 3.6(3) × $10^{-5}$ $s^{-1}$ |

[a]Conditions: toluene-$d_8$, 298 K, 10-fold excess of benzyl chloride.

the rate constants as a function of the nucleophilic metal (Fe vs Ru), the Fp derivative exhibited rate constants 17−25 times larger than the Rp derivative for both the trifluoromethyl- and cyano-substituted benzyl chloride substrates. Given the wide range of nucleophilicities exhibited by metal carbonyl anions generally (ranging over 8 orders of magnitude),[74] the observed trends in Table 2 are quite similar to the established trends for $[Fp]^-$ versus $[Rp]^-$. We consider this to be an indication that the known reaction rates of the bare $[M]^-$ metal carbonyl anions can be used to predict relative reactivities of heterobimetallic (NHC)Cu-[M] complexes with the same NHC ligand, to within an order of magnitude. The (IPr)Cu-$WCp(CO)_3$ derivative, whose metal carbonyl anion is 7 × $10^{-6}$ times less nucleophilic than $[Fp]^-$, did not react even with *p*-cyanobenzyl chloride under these conditions.

We also were interested in periodic trends with regard to the group 11 metal in the heterobimetallic pair. To understand this effect, we synthesized (IPr)Ag-Fp and (IPr)Au-Fp by reaction of $[Fp]^-$ with the corresponding metal chloride precursors. The solid-state structures (Figure 3) of both species are

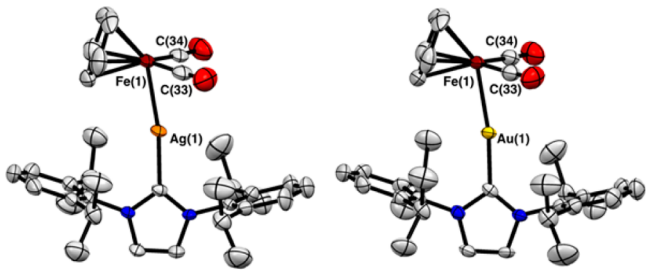


**Figure 3.** Solid-state structures of (IPr)Ag-Fp (left) and (IPr)Au-Fp (right) determined by X-ray crystallography. Atoms are depicted as 50% probability thermal ellipsoids. Hydrogen atoms and cocrystallized toluene molecules have been omitted. Selected bond distances (Å): Ag(1)−Fe(1), 2.5215(11); Ag(1)−C(33), 2.80(1); Ag(1)−C(34), 2.768(8); Au(1)−Fe(1), 2.5059(7); Au(1)−C(33), 2.808(7); Au(1)−C(34), 2.780(7).

topologically similar to the known structure of (IPr)Cu-Fp.[67] The M−Fe distances in the (IPr)M-Fp series follow the expected trend down the triad (Cu−Fe, 2.3462(5) Å; Ag−Fe, 2.5215(11) Å; Au−Fe, 2.5059(7) Å) and, when correcting for the size of the metals, have essentially identical formal shortness ratios[75] (Cu−Fe, 1.004; Ag−Fe, 1.007; Au−Fe, 1.002). While (IPr)Cu-Fp contains two semibridging carbonyl ligands


DOI: 10.1021/acs.organomet.5b00476
*Organometallics* 2015, 34, 3857−3864

according to calculations of their asymmetry parameters,[76] (IPr)Ag-Fp has two CO ligands that are borderline cases between semibridging and terminal, and (IPr)Au-Fp has one borderline CO and one terminal CO.[77]

Neither (IPr)Ag-Fp nor (IPr)Au-Fp was observed to react with benzyl chloride at room temperature, indicating that the effect of moving down the group 11 triad is to significantly decrease the rate of alkyl halide BOA. This may be related to the increasing covalency of M−Fe bonding down the triad that is expected because of the increasing radial extent of the d-orbitals and the increasing electronegativity of the group 11 metals. Evidence for this increasing M−Fe covalency can be found both experimentally and computationally (Table 3).

**Table 3. Selected Experimental and Computational Parameters for (NHC)M-Fp (M = Cu, Ag, Au)[a]**

| complex | experimental $\nu_{CO}$ ($cm^{-1}$) | calculated $\nu_{CO}$ ($cm^{-1}$) | M−Fe WBI[b] | M−Fe $\Delta q$[c] |
|---|---|---|---|---|
| (NHC)Cu-Fp[d] | 1914, 1849 | 1926, 1875 | 0.39 | 1.58 |
| (NHC)Ag-Fp | 1916, 1853 | 1936, 1891 | 0.42 | 1.53 |
| (NHC)Au-Fp | 1933, 1872 | 1953, 1909 | 0.48 | 1.45 |

[a]NHC = IPr for experimental data and IMe = *N*,*N*′-dimethylimidazol-2-ylidene for computational data. [b]Wiberg bond index from NBO calculations. [c]Calculated difference in natural charge between M and Fe. [d]Data from ref 67.

Experimentally, we observe that the $\nu_{CO}$ values for the $[Fp]^-$ fragment measured by FT-IR increase from (IPr)Cu-Fp to (IPr)Ag-Fp to (IPr)Au-Fp. The $\nu_{CO}$ values calculated by DFT reproduce this trend. The increasing $\nu_{CO}$ values likely are indicative of a less electron-rich Fe center as the M−Fe bonding becomes less ionic and more covalent down the triad. The Wiberg bond indices from NBO calculations also indicate an increasing degree of M−Fe covalency down the triad. Lastly, the M−Fe bond polarity from natural charge calculations also indicates decreasing ionic character down the triad. We should also note that the decrease in BOA reaction rate when moving from Cu to Ag and Au may relate to the less efficient semibridging M···CO interactions for the heavier congeners, as the computational studies described below indicate a possible role for bridging carbonyls in the BOA transition state.

**Computational Transition-State Characterization.** In order to examine the heterobimetallic reaction computationally, we chose to begin with gas-phase DFT calculations at the BVP86/LANL2TZ(f) level of theory on the model reaction between the reactants (IMe)Cu-Fp + $CH_3Cl$ to yield products (IMe)Cu-Cl + Fp-$CH_3$ (IMe = *N*,*N*′-dimethylimidazol-2-ylidene). The overall reaction was calculated to be exergonic by $\Delta G_{298\ K}$ = −20.0 kcal/mol. A transition state (**TS1**) for this reaction was identified computationally as lying higher in energy by $\Delta G_{298\ K}^{\ddagger}$ = +26.2 kcal/mol than the individual reactants. A surprisingly good match was found between the calculated activation parameters for the (IMe)Cu-Fp + $CH_3Cl$ reaction ($\Delta H^{\ddagger}$ = +14.6 kcal/mol; $\Delta S^{\ddagger}$ = −39.0 eu) and the experimental ones for the (IPr)Cu-Fp + benzyl chloride reaction ($\Delta H^{\ddagger}$ = +13(2) kcal/mol; $\Delta S^{\ddagger}$ = −36(7) eu). When benzene solvation was included in the calculations, these energetics differed by only ∼2 kcal/mol compared to the gas-phase values, and so gas-phase calculations were utilized subsequently. The calculated energetics of this pathway are consistent with the experimental observation of the reaction occurring at ambient conditions. For comparison, an alternative mechanism would involve ionization of the Cu−Fe bond to reveal $[Fp]^-$, which could then react with the alkyl halide by the known $S_N2$ pathway.[70] We have previously calculated that the $[(IMe)Cu]^+[Fp]^-$ ion pair is higher in energy by >80 kcal/mol than neutral (IMe)Cu-Fp in benzene solution, i.e., too high in energy to be accessible under ambient conditions.[66] This fact, combined with the phenomenological observations detailed above regarding product profiles, causes us to rule out this alternative pathway, as it is inconsistent with experimental observations.

The structure of **TS1** (Figure 4) results from approach of $CH_3Cl$ toward a point between Cu and Fe along a trajectory

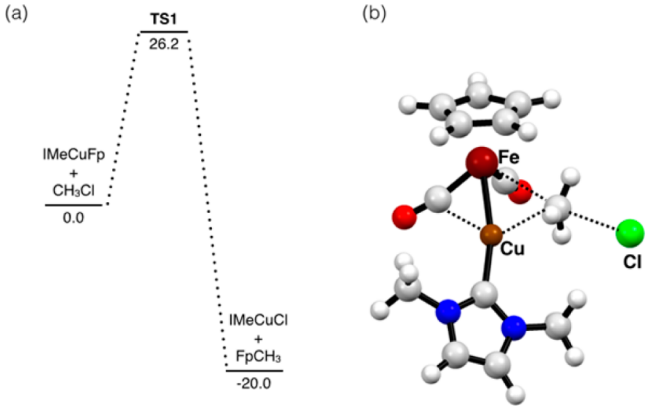


**Figure 4.** (a) Calculated reaction coordinate diagram for reactants (IMe)Cu-Fp + $CH_3Cl$ to products (IMe)Cu-Cl + Fp-$CH_3$, with relative free energies given in kcal/mol at 298 K. (b) Structure of **TS1**.

that bisects one of the Cp(centroid)−Fe−CO angles. The C−Cl bond is almost fully broken (2.45 Å) relative to the calculated C−Cl distance in free $CH_3Cl$ (1.84 Å). The $[CH_3]$ unit is planar, resembling the stereoinvertive transition-state structure of a typical $S_N2$ reaction. The Cu−Fe bond is intact but slightly elongated (2.41 Å) relative to the reactant structure (2.33 Å). The Cu···CO interaction nearest to the incoming $CH_3Cl$ molecule is elongated (2.94 Å) relative to the reactant structure (2.57 Å), while the Cu···CO interaction on the face opposite the incoming $CH_3Cl$ molecule is contracted (2.22 Å) relative to the reactant structure (2.49 Å). Because no new Cu−CO bond ultimately forms in the products, this latter Cu···CO contraction in **TS1** highlights the templating role played by that CO ligand, holding the bimetallic transition-state structure together as the Cu−Fe bond breaks. The Fe−$CH_3$ bond is only slightly formed (2.85 Å) relative to the calculated distance in the Fp-$CH_3$ product (2.05 Å). The $[CH_3]$ carbon also engages in a close Cu···C contact (2.19 Å) despite the fact that no new Cu−C bond forms in the products, indicating that the Cu center plays an important role in the transition state, as well.

NBO calculations on **TS1** were carried out to analyze how both natural charge distribution and bonding interactions change during the reaction pathway. For comparative purposes (see Figure 4a), we also present these data for the reactants and products.

Selected natural charge data are compiled in Table 4. Consistent with the formally BOA process, the [Fp] fragment is oxidized during the reaction. As we have noted before,[66,68] within the [Fp] fragment the redox chemistry is dominated by


DOI: 10.1021/acs.organomet.5b00476
*Organometallics* 2015, 34, 3857−3864

**Table 4. Calculated Natural Charges along the Reaction Coordinate**

| complex | $q$(IMeCu) | $q$(Fp) | $q$(2CO) | $q$($CH_3$) | $q$(Cl) |
|---|---|---|---|---|---|
| reactants | 0.62 | −0.62 | 0.39 | 0.08 | −0.08 |
| **TS1** | 0.28 | −0.28 | 0.48 | 0.10 | −0.50 |
| products | 0.52 | 0.01 | 0.72 | −0.01 | −0.52 |

the CO ligands (Table 4) and Cp ligand, and the natural charge on Fe is relatively constant (between $q$ = −1.17 and −1.00) throughout the reaction pathway. Regarding the $CH_3Cl$ molecule undergoing BOA, there is essentially no change in natural charge residing on the [$CH_3$] unit. The chloride, however, experiences dramatic ionization at **TS1** and remains largely anionic in character in the (IMe)Cu-Cl product.

Selected Wiberg and Mayer bond index data are compiled in Table 5. As expected, the $CH_3Cl$ carbon experiences a smooth

**Table 5. Selected Wiberg and Mayer Bond Index Values along the Reaction Coordinate**[a]

| complex | Cu−C(methyl) | Fe−C(methyl) | Cu−C(proximal CO)[b] | Cu−C(distal CO)[b] |
|---|---|---|---|---|
| reactants | | | 0.13/0.13 | 0.15/0.15 |
| **TS1** | 0.25/0.25 | 0.31/0.31 | 0.07/0.07 | 0.26/0.26 |
| products | | 0.71/0.71 | | |

[a]Values are given as Wiberg/Mayer. [b]Proximal and distal refer to the position of a CO ligand relative to the incoming $CH_3Cl$ molecule.

increase in bonding interaction with the Fe center during the reaction. Of particular note is that while a Cu−$CH_3$ bond does not form in the products, there is a significant Cu−$CH_3$ interaction in **TS1** of equal magnitude to the Fe−$CH_3$ interaction. This observation indicates that **TS1** is a true bimetallic transition state, where both Cu and Fe interact with the BOA substrate equally. As expected because the [(IMe)Cu] and [Fp] fragments are separating in this reaction, the Cu···CO interaction with the carbonyl group proximal to the incoming $CH_3Cl$ substrate experiences a smooth decrease during the reaction. Of particular note is the Cu···CO interaction distal to the incoming $CH_3Cl$ molecule. Whereas this semibridging Cu···CO interaction in (IMe)Cu-Fp ultimately breaks, the interaction is actually amplified in **TS1**. In other words, the distal semibridging CO ligand bridges the Cu−Fe bond more significantly in the transition state than in either the reactants or the products. This observation indicates that, in addition to playing an important role in the redox changes during BOA and BRE (see above),[66,68] the semibridging CO ligands also play a key structural role, essentially templating the bimetallic transition state to stabilize it as the metal−metal bond is breaking.

Lastly, we attempted to study transition states related to **TS1** with various *para*-substituted benzyl chloride substrates in place of $CH_3Cl$. A similar transition state, **TS2-H**, was located for the parent benzyl chloride, with a similar barrier height to that for $CH_3Cl$ ($\Delta G_{298\ K}^{\ddagger}$ = +28.6 kcal/mol) and with similar activation parameters ($\Delta H^{\ddagger}$ = +15.8 kcal/mol; $\Delta S^{\ddagger}$ = −43.0 eu). Transition states also were located for benzyl chloride substrates with cyano, methyl, and methoxy substituents in the *para* position (**TS2-CN**, **TS2-Me**, **TS2-OMe**). Unlike the experimentally determined Hammett reaction constant of $\rho$ = 1.6(2), the barrier heights corresponding to **TS2-H**, **TS2-CN**, **TS2-Me**, and **TS2-OMe** were very similar (between +27.1 and +28.6 kcal/mol), indicating a Hammett constant close to zero. When conducting the calculations with a different DFT functional (B3LYP instead of BVP86) or when including implicit benzene solvation, the absolute values of the energies changed, but the collective trend remained unchanged. While this inability to reproduce a kinetic parameter in the BOA reaction is likely reflective of the various sources of error associated with quantitatively correlating computational mechanisms to experimental rate constants (especially regarding entropic contributions to highly polarized systems such as this one),[78,79] we are nonetheless confident in the ability of our model to qualitatively reveal the detailed nature of the BOA transition state highlighted in the discussion of **TS1** above.

## CONCLUSIONS

In conclusion, the transition state for alkyl halide BOA by (IPr)Cu-Fp and related complexes has been thoroughly characterized by both experimental and computational methods. Cyclopropylmethyl halide substrates were used to indicate the limitations of assuming a two-electron BOA pathway without long-lived radical intermediates. Eyring analysis was used to measure activation parameters for the reaction between (IPr)Cu-Fp and benzyl chloride, indicating a large and negative entropy of activation consistent with a highly organized transition state. Hammett analysis was used to determine the electronic bias of the reaction pathway, indicating a buildup of negative charge in the transition state on the alkyl halide carbon. Substituting Fe for Ru results in an order of magnitude decrease in reaction rate, consistent with previous observations for the free $[Fp]^-$ and $[Rp]^-$ anions themselves. Substituting Cu for Ag or Au results in a dramatic decrease in reaction rate, possibly indicating that more covalent M−Fe bonds are less reactive toward alkyl halide BOA. Computational analysis revealed important features of the transition state unavailable from experimental data, including the dual role of the carbonyl ligands in the [Fp] group both of acting as redox noninnocent ligands during the BOA reaction and also of providing structural stability to the transition state as the metal−metal bond breaks.

## EXPERIMENTAL SECTION

**General Considerations.** All reactions and manipulations were conducted under purified $N_2$ using standard Schlenk line techniques or in a glovebox. Glassware was oven-dried prior to use. Bulk reaction solvents were purified using a Glass Contours Solvent System built by Pure Process Technology, LLC. Deuterated solvents were degassed by repeated freeze−pump−thaw cycles and stored over activated 3 Å molecular sieves prior to use. $^1H$ and $^{13}C$ NMR spectra were recorded using Bruker Avance 400 MHz or 500 MHz NMR spectrometers. NMR spectra were recorded at room temperature unless otherwise indicated, and chemical shifts were referenced to residual solvent peaks. FT-IR spectra were recorded in a glovebox on powder samples using a Bruker ALPHA spectrometer fitted with a diamond-ATR detection unit. Elemental analyses were performed by Midwest Microlab, LLC, in Indianapolis, IN, USA. Single-crystal X-ray diffraction studies were performed using a Bruker SMART X2S benchtop diffractometer fitted with an Oxford Cryostreams desktop cooler. Solution and refinement were accomplished with the SHELXTL suite of programs,[80] using standard methods,[81] and CIF files are included as Supporting Information. Literature methods were used to synthesize KFp,[82] (IPr)Cu-Fp,[67] (IPr)Cu-Rp,[77] (IPr)Ag-Cl,[83] and (IPr)Au-Cl.[84] All other reagents were purchased from commercial vendors.

**Kinetics Measurements.** Stock solutions of (IPr)Cu-Fp (16 mM) and mesitylene (79 mM) were made in toluene-$d_8$. Prior to each



DOI: 10.1021/acs.organomet.5b00476
*Organometallics* 2015, 34, 3857−3864

individual experiment, the (IPr)Cu-Fp solution (500 μL) and the mesitylene solution (100 μL) were combined, and the appropriate benzyl chloride (10 equiv relative to IPrCuFp) was added. The resulting solution was mixed, filtered, and transferred to a J. Young NMR tube. The tube was removed from the glovebox and placed in a −78 °C bath until ready for use. In order to obtain rate data, the tube was placed in an NMR probe preset to the appropriate temperature and allowed to equilibrate. The initial disappearance (over approximately 2800−5800 s) of (IPr)Cu-Fp was monitored by following the more downfield isopropyl doublet, the isopropyl septet, and the cyclopentadienyl singlet (unless peak overlap precluded monitoring of one or more of these resonances). Early data points reflective of temperature equilibration or other instrumental artifacts were deleted manually (typically ∼2% of all data points). The resulting data were fit to the kinetic model in eq 1, where $A_t$ is the integrated area of the (IPr)Cu-Fp resonance of interest (normalized to the mesitylene standard) at time $t$, $A_0$ is the initial integrated area of that resonance, and $k$ is the pseudo-first-order rate constant. Each reported rate constant results from averaging over each of the resonances listed above across multiple experimental runs, and error bars were calculated using standard error propagation. For cases where a large variance was observed between duplicate runs, we consider contamination by trace amounts of air and small deviations in sample concentrations to be the likeliest sources of error.

$$A_t = A_0 e^{-kt} \quad (1)$$

**Preparation of (IPr)Ag-Fp.** (IPr)AgCl (0.3670 g, 0.670 mmol, 1 equiv) was dissolved in toluene (10 mL), and KFp (0.2981 g, 1.38 mmol, 2 equiv) was added to the solution. The brown solution was stirred for 16 h at room temperature. The solution was filtered through Celite, and the filtrate was evaporated to dryness. The remaining solid was suspended in pentane (10 mL) and stirred vigorously for 30 min. The suspension was filtered through a fritted glass filter, and the yellow solid was washed with pentane (3 × 5 mL) and then dried *in vacuo*. Yield: 0.2705 g, 0.402 mmol, 58%. The solid was stored in a glovebox freezer at −36 °C. X-ray quality crystals were grown by vapor diffusion of pentane into a concentrated toluene solution at −36 °C. $^1$H NMR (500 MHz, $C_6D_6$): $\delta$ 7.20 (t, $^3J_{HH}$ = 7.8 Hz, 2H, *p*-CH), 7.08 (d, $^3J_{HH}$ = 7.7 Hz, 4H, *m*-CH), 6.31 (d, $^4J_{AgH}$ = 1.1 Hz, 2H, NCH), 4.30 (s, Cp), 2.60 (sept., $^3J_{HH}$ = 6.8 Hz, 4H, C$\underline{H}$(CH$_3$)$_2$), 1.45 (d, $^3J_{HH}$ = 6.7 Hz, 12H, CH(C$\underline{H}_3$)$_2$), 1.09 (d, $^3J_{HH}$ = 6.9 Hz, 12H, CH(C$\underline{H}_3$)$_2$). $^{13}$C{$^1$H} NMR (125 MHz, $C_6D_6$): $\delta$ 221.7 (CO), 145.7, 135.0, 130.4, 124.0, 121.9, 76.5 (Cp), 28.7, 24.5, 23.6. Note: Even after 10 000 scans on a near-saturated solution, the $^{13}$C signal for the carbene carbon was not detected. IR (solid, cm$^{-1}$): 3148, 3098, 3061, 2961, 2928, 2866, 1915 ($\nu_{CO}$), 1852 ($\nu_{CO}$), 1457, 1406, 1326, 1106, 1058, 802, 757, 654, 587, 502. Anal. Calcd for $C_{34}H_{41}AgFeN_2O_2$: C, 60.64; H, 6.14; N, 4.16. Found: C, 60.74; H, 6.25; N, 4.25.

**Preparation of (IPr)Au-Fp.** (IPr)AuCl (0.0526 g, 0.085 mmol, 1 equiv) was dissolved in toluene (10 mL), and KFp (0.0366 g, 0.169 mmol, 2 equiv) was added to the solution. The brown solution was stirred at room temperature for 16 h. The solution was filtered through Celite, and the filtrate was evaporated to dryness. The remaining solid was suspeneded in pentane (10 mL) and stirred vigorously for 30 min. The suspension was filtered through a fritted glass filter, and the yellow solid was washed with pentane (3 × 5 mL) and then dried *in vacuo*. Yield: 0.0505 g, 0.0662 mmol, 82%. The solid was stored in a glovebox freezer at −36 °C. X-ray quality crystals were grown by vapor diffusion of pentane into a concentrated toluene solution at −36 °C. $^1$H NMR (500 MHz, $C_6D_6$): $\delta$ 7.22 (t, $^3J_{HH}$ = 7.7 Hz, 2H, *p*-CH), 7.10 (d, $^3J_{HH}$ = 7.7 Hz, 4H, *m*-CH), 6.29 (s, 2H, NCH), 4.26 (s, Cp), 2.68 (sept., $^3J_{HH}$ = 6.7 Hz, 4H, C$\underline{H}$(CH$_3$)$_2$), 1.57 (d, $^3J_{HH}$ = 6.9 Hz, 12H, CH(C$\underline{H}_3$)$_2$), 1.12 (d, $^3J_{HH}$ = 6.9 Hz, 12H, CH(C$\underline{H}_3$)$_2$). $^{13}$C{$^1$H} NMR (125 MHz, $C_6D_6$): $\delta$ 218.4 (CO), 195.4 (NCCu), 146.0, 135.0, 130.6, 124.2, 121.4, 78.7 (Cp), 29.1, 24.5, 24.1. IR (solid, cm$^{-1}$): 3150, 3102, 3068, 2960, 2929, 2865, 1933 ($\nu_{CO}$), 1872 ($\nu_{CO}$), 1593, 1468, 1456, 1412, 1326, 1102, 1058, 1012, 816, 802, 758, 747, 650, 601, 582, 547. Anal. Calcd for $C_{34}H_{41}AuFeN_2O_2$: C, 53.56; H, 5.42; N, 3.67. Found: C, 53.57; H, 5.52; N, 3.68.

**Computational Methods.** All calculations were performed using Gaussian09, Revision B.01.[85] Density functional theory (DFT) calculations were carried out using a hybrid functional, BVP86, consisting of Becke's 1988 gradient-corrected Slater exchange functional[86] combined with the VWNS local electron correlation functional and Perdew's 1986 nonlocal electron correlation functional.[87] Mixed basis sets were employed for the smaller MeCl system: the LANL2TZ(f) triple-$\zeta$ basis set[88−90] with effective core potential[88,91,92] was used for Cu, Ag, Au, and Fe; the LANL2DZ double-$\zeta$ basis set with effective core potential was used for Cl; and the Gaussian09 internal 6-311+G(d) basis set was used for C, H, N, and O. All geometry optimizations were performed using LANL2DZ effective core potentials (ECP) for the larger systems with BnCl and BnCl derivatives. Single-point electronic energy calculations were then carried out using larger mixed basis sets: the LANL2TZ(f) triple-$\zeta$ basis set with effective core potential for Cu and Fe, the LANL2DZ double-$\zeta$ basis set with effective core potential for Cl, and the Gaussian09 internal 6-311+G(d) basis set for C, H, N, and O. In some cases, effects of solvation by benzene were calculated with the polarizable continuum model (PCM) using the integral equation formalism variant (IEFPCM)[93] with default settings as implemented in Gaussian09. The 2,6-diisopropylphenyl groups on the NHC ligands were truncated to methyl groups in order to minimize computational time. Vibrational frequency analysis confirmed that all stationary points were correctly identified either as stable intermediates with zero imaginary frequencies or transition states with only one imaginary frequency. Intrinsic reaction coordinate calculations confirmed that each transition state was situated between its corresponding reactant and product states on the Born−Oppenheimer potential energy surface. Natural population analysis was used to determine atomic and fragment charges, and Wiberg and Mayer bond indices were used to determine bond orders: both were obtained from NBO v. 3.1[94] calculations within Gaussian09.

## ■ ASSOCIATED CONTENT

### Supporting Information

Spectral data, computational output, crystallographic CIF files. The Supporting Information is available free of charge on the ACS Publications website at DOI: 10.1021/acs.organomet.5b00476.

## ■ AUTHOR INFORMATION


### Corresponding Author

*E-mail: npm@uic.edu.

### Author Contributions

†M. K. Karunananda and S. R. Parmelee contributed equally.


### Notes

The authors declare no competing financial interest.

## ■ ACKNOWLEDGMENTS


Funding was provided by the National Science Foundation (CHE-1362294) and the UIC Department of Chemistry. Dr. Dan McElheny assisted with NMR spectroscopy. Dr. Frank Vázquez assisted with DFT calculations. Computational resources were provided by the Extreme Computing cluster at UIC. Dr. Bernard Santarsiero assisted with X-ray crystallography analysis. The authors would like to thank the reviewers of the manuscript for insightful suggestions.


## ■ REFERENCES


(1) Buchwalter, P.; Rosé, J.; Braunstein, P. *Chem. Rev.* **2015**, *115*, 28−126.

(2) Cooper, B. G.; Napoline, J. W.; Thomas, C. M. *Catal. Rev.: Sci. Eng.* **2012**, *54*, 1−40.

(3) Gade, L. H. *Angew. Chem., Int. Ed.* **2000**, *39*, 2658−2678.




DOI: 10.1021/acs.organomet.5b00476
*Organometallics* 2015, 34, 3857−3864

(4) Pérez-Temprano, M. H.; Casares, J. A.; Espinet, P. *Chem. - Eur. J.* **2012**, *18*, 1864−1884.
(5) Bruno, G.; Schiavo, L. S.; Rotondo, E.; Arena, C. G. *Organometallics* **1989**, *8*, 886−892.
(6) Ariafard, A.; Hyland, C. J. T.; Canty, A. J.; Sharma, M.; Yates, B. F. *Inorg. Chem.* **2011**, *50*, 6449−6457.
(7) Walker, W. K.; Kay, B. M.; Michaelis, S. A.; Anderson, D. L.; Smith, S. J.; Ess, D. H.; Michaelis, D. J. *J. Am. Chem. Soc.* **2015**, *137*, 7371−7378.
(8) Yin, G.; Kalvet, I.; Schoenebeck, F. *Angew. Chem.* **2015**, *127*, 6913−6917.
(9) Pei, X.-L.; Yang, Y.; Lei, Z.; Chang, S.-S.; Guan, Z.-J.; Wan, X.-K.; Wen, T.-B.; Wang, Q.-M. *J. Am. Chem. Soc.* **2015**, *137*, 5520−5525.
(10) Zhang, Y.; Roberts, S. P.; Bergman, R. G.; Ess, D. H. *ACS Catal.* **2015**, *5*, 1840−1849.
(11) Klähn, M.; Garland, M. V. *ACS Catal.* **2015**, *5*, 2301−2316.
(12) Sterenberg, B. T.; Wrigley, C. T.; Puddephatt, R. J. *Dalton Trans.* **2015**, *44*, 5555−5568.
(13) Powers, D. C.; Anderson, B. L.; Hwang, S. J.; Powers, T. M.; Pérez, L. M.; Hall, M. B.; Zheng, S.-L.; Chen, Y.-S.; Nocera, D. G. *J. Am. Chem. Soc.* **2014**, *136*, 15346−15355.
(14) Romashov, L. V.; Khemchyan, L. L.; Gordeev, E. G.; Koshevoy, I. O.; Tunik, S. P.; Ananikov, V. P. *Organometallics* **2014**, *33*, 6003−6012.
(15) Adams, R. D.; Rassolov, V.; Wong, Y. O. *Angew. Chem., Int. Ed.* **2014**, *53*, 11006−11009.
(16) Levin, M. D.; Toste, F. D. *Angew. Chem., Int. Ed.* **2014**, *53*, 6211−6215.
(17) Anand, M.; Sunoj, R. B.; Schaefer, H. F., III. *J. Am. Chem. Soc.* **2014**, *136*, 5535−5538.
(18) Wolf, W. J.; Winston, M. S.; Toste, F. D. *Nat. Chem.* **2013**, *6*, 159−164.
(19) Sabater, S.; Mata, J. A.; Peris, E. *Nat. Commun.* **2013**, *4*, 1−7.
(20) Choy, S. W. S.; Page, M. J.; Bhadbhade, M.; Messerle, B. A. *Organometallics* **2013**, *32*, 4726−4729.
(21) Bonney, K. J.; Proutiere, F.; Schoenebeck, F. *Chem. Sci.* **2013**, *4*, 4434−4439.
(22) Takahashi, K.; Yamashita, M.; Nozaki, K. *J. Am. Chem. Soc.* **2012**, *134*, 18746−18757.
(23) Hirner, J. J.; Roth, K. E.; Shi, Y.; Blum, S. A. *Organometallics* **2012**, *31*, 6843−6850.
(24) Bauer, J.; Braunschweig, H.; Damme, A.; Radacki, K. *Angew. Chem., Int. Ed.* **2012**, *51*, 10030−10033.
(25) Kure, B.; Taniguchi, A.; Nakajima, T.; Tanase, T. *Organometallics* **2012**, *31*, 4791−4800.
(26) Oishi, M.; Kino, M.; Saso, M.; Oshima, M.; Suzuki, H. *Organometallics* **2012**, *31*, 4658−4661.
(27) González-Pérez, A. B.; Álvarez, R.; Faza, O. N.; de Lera, Á. R.; Aurrecoechea, J. M. *Organometallics* **2012**, *31*, 2053−2058.
(28) Teets, T. S.; Nocera, D. G. *J. Am. Chem. Soc.* **2011**, *133*, 17796−17806.
(29) Teets, T. S.; Neumann, M. P.; Nocera, D. G. *Chem. Commun.* **2011**, *47*, 1485.
(30) Powers, D. C.; Benitez, D.; Tkatchouk, E.; Goddard, W. A., III; Ritter, T. *J. Am. Chem. Soc.* **2010**, *132*, 14092−14103.
(31) Powers, D. C.; Ritter, T. *Nat. Chem.* **2009**, *1*, 302−309.
(32) Covell, D. J.; White, M. C. *Angew. Chem., Int. Ed.* **2008**, *47*, 6448−6451.
(33) Reed, S. A.; White, M. C. *J. Am. Chem. Soc.* **2008**, *130*, 3316−3318.
(34) Hassan, M. R.; Hogarth, G.; Golzar Hossain, G. M.; Kabir, S. E.; Raha, A. K.; Saha, M. S.; Tocher, D. A. *Organometallics* **2007**, *26*, 6473−6480.
(35) Gautron, S.; Lassauque, N.; Le Berre, C.; Azam, L.; Giordano, R.; Serp, P.; Laurenczy, G.; Daran, J.-C.; Duhayon, C.; Thiébaut, D.; Kalck, P. *Organometallics* **2006**, *25*, 5894−5905.
(36) Yoshikai, N.; Yamanaka, M.; Ojima, I.; Morokuma, K.; Nakamura, E. *Organometallics* **2006**, *25*, 3867−3875.
(37) Hilts, R. W.; Oke, O.; Ferguson, M. J.; McDonald, R.; Cowie, M. *Organometallics* **2005**, *24*, 4393−4405.
(38) Cui, W.; Wayland, B. B. *J. Am. Chem. Soc.* **2004**, *126*, 8266−8274.
(39) Stockland, R. A.; Janka, M.; Hoel, G. R.; Rath, N. P.; Anderson, G. K. *Organometallics* **2001**, *20*, 5212−5219.
(40) Heyduk, A. F.; Nocera, D. G. *Science* **2001**, *293*, 1639−1641.
(41) Hanna, T. A.; Baranger, A. M.; Bergman, R. G. *J. Am. Chem. Soc.* **1995**, *117*, 11363−11364.
(42) Ciriano, M. A.; Jesfis, J.; Lahoz, F. J.; Oro, L. A. *J. Organomet. Chem.* **1994**, *482*, 53−62.
(43) Broussard, M. E.; Juma, B.; Train, S. G.; Peng, W.-J.; Laneman, S. A.; Stanley, G. G. *Science* **1993**, *260*, 1784−1788.
(44) Beck, W.; Raab, K.; Nagel, U.; Sacher, W. *Angew. Chem., Int. Ed. Engl.* **1985**, *24*, 505−506.
(45) Schenck, T. G.; Milne, C.; Sawyer, J.; Bosnich, B. *Inorg. Chem.* **1985**, *24*, 2338−2344.
(46) Coleman, A. W.; Eadie, D. T.; Stobart, S. R. *J. Am. Chem. Soc.* **1982**, *104*, 922−923.
(47) Tkatchouk, E.; Mankad, N. P.; Benitez, D.; Goddard, W. A.; Toste, F. D. *J. Am. Chem. Soc.* **2011**, *133*, 14293−14300.
(48) Fackler, J. P. *Inorg. Chem.* **2002**, *41*, 6959−6972.
(49) van der Vlugt, J. I. *Eur. J. Inorg. Chem.* **2012**, *2012*, 363−375.
(50) Breitenfeld, J.; Ruiz, J.; Wodrich, M. D.; Hu, X. *J. Am. Chem. Soc.* **2013**, *135*, 12004−12012.
(51) Ahmed, S. M.; Poater, A.; Childers, M. I.; Widger, P. C. B.; LaPointe, A. M.; Lobkovsky, E. B.; Coates, G. W.; Cavallo, L. *J. Am. Chem. Soc.* **2013**, *135*, 18901−18911.
(52) Huang, W.; Dulong, F.; Khan, S. I.; Cantat, T.; Diaconescu, P. L. *J. Am. Chem. Soc.* **2014**, *136*, 17410−17413.
(53) Rabinowitz, H. N.; Karlin, K. D. *J. Am. Chem. Soc.* **1977**, *99*, 1420−1426.
(54) Bauer, G.; Wodrich, M. D.; Scopelliti, R.; Hu, X. *Organometallics* **2015**, *34*, 289−298.
(55) Gavrilova, A. L.; Qin, C. J.; Sommer, R. D.; Rheingold, A. L.; Bosnich, B. *J. Am. Chem. Soc.* **2002**, *124*, 1714−1722.
(56) Grant, D. J.; Stewart, T. J.; Bau, R.; Miller, K. A.; Mason, S. A.; Gutmann, M.; McIntyre, G. J.; Gagliardi, L.; Evans, W. J. *Inorg. Chem.* **2012**, *51*, 3613−3624.
(57) Crowley, J. D.; Goldup, S. M.; Gowans, N. D.; Leigh, D. A.; Ronaldson, V. E.; Slawin, A. M. Z. *J. Am. Chem. Soc.* **2010**, *132*, 6243−6248.
(58) Yuan, J.; Wang, J.; Zhang, G.; Liu, C.; Qi, X.; Lan, Y.; Miller, J. T.; Kropf, A. J.; Bunel, E. E.; Lei, A. *Chem. Commun.* **2015**, *51*, 576−579.
(59) Schley, N. D.; Fu, G. C. *J. Am. Chem. Soc.* **2014**, *136*, 16588−16593.
(60) Marquard, S. L.; Bezpalko, M. W.; Foxman, B. M.; Thomas, C. M. *J. Am. Chem. Soc.* **2013**, *135*, 6018−6021.
(61) Steiman, T. J.; Uyeda, C. *J. Am. Chem. Soc.* **2015**, *137*, 6104−6110.
(62) Trinquier, G.; Hoffmann, R. *Organometallics* **1984**, *3*, 370−380.
(63) Mazzacano, T. J.; Mankad, N. P. *J. Am. Chem. Soc.* **2013**, *135*, 17258−17261.
(64) Mkhalid, I. A. I.; Barnard, J. H.; Marder, T. B.; Murphy, J. M.; Hartwig, J. F. *Chem. Rev.* **2010**, *110*, 890−931.
(65) Mazzacano, T. J.; Mankad, N. P. *Chem. Commun.* **2015**, *51*, 5379−5382.
(66) Parmelee, S. R.; Mazzacano, T. J.; Zhu, Y.; Mankad, N. P.; Keith, J. A. *ACS Catal.* **2015**, *5*, 3689−3699.
(67) Jayarathne, U.; Mazzacano, T. J.; Bagherzadeh, S.; Mankad, N. P. *Organometallics* **2013**, *32*, 3986−3992.
(68) Karunananda, M. K.; Vázquez, F. X.; Alp, E. E.; Bi, W.; Chattopadhyay, S.; Shibata, T.; Mankad, N. P. *Dalton Trans.* **2014**, *43*, 13661.
(69) Bowry, V. W.; Lusztyk, J.; Ingold, K. U. *J. Am. Chem. Soc.* **1991**, *113*, 5687−5698.
(70) Theys, R.; Dudley, M.; Hossain, M. *Coord. Chem. Rev.* **2009**, *253*, 180−234.


DOI: 10.1021/acs.organomet.5b00476
*Organometallics* 2015, 34, 3857−3864

(71) Krusic, P. J.; Fagan, P. J.; San Filippo, J., Jr. *J. Am. Chem. Soc.* **1977**, *99*, 250−252.
(72) Whitesides, G. M.; Boschetto, D. J. *J. Am. Chem. Soc.* **1969**, *91*, 4313−4314.
(73) Bock, P. L.; Boschetto, D. J.; Rasmussen, J. R.; Demers, J. P.; Whitesides, G. M. *J. Am. Chem. Soc.* **1974**, *96*, 2814−2825.
(74) King, R. B. *Acc. Chem. Res.* **1970**, *3*, 417−427.
(75) Cotton, F. A.; Daniels, L. M.; Murillo, C. A.; Zhou, H. C. *Inorg. Chim. Acta* **2000**, *300*−*302*, 319−327.
(76) Curtis, M. D.; Han, K. R.; Butler, W. M. *Inorg. Chem.* **1980**, *19*, 2096−2101.
(77) Banerjee, S.; Karunananda, M. K.; Bagherzadeh, S.; Jayarathne, U.; Parmelee, S. R.; Waldhart, G. W.; Mankad, N. P. *Inorg. Chem.* **2014**, *53*, 11307−11315.
(78) Plata, R. E.; Singleton, D. A. *J. Am. Chem. Soc.* **2015**, *137*, 3811−3826.
(79) Winter, A. *Nat. Chem.* **2015**, *7*, 473−475.
(80) Sheldrick, G. M. *Acta Crystallogr., Sect. A: Found. Crystallogr.* **2008**, *64*, 112−122.
(81) Müller, P. *Crystallogr. Rev.* **2009**, *15*, 57−83.
(82) Ohishi, T.; Shiotani, Y.; Yamashita, M. *J. Org. Chem.* **1994**, *59*, 250−250.
(83) de Frémont, P.; Scott, N. M.; Stevens, E. D.; Ramnial, T.; Lightbody, O. C.; Macdonald, C. L. B.; Clyburne, J. A. C.; Abernethy, C. D.; Nolan, S. P. *Organometallics* **2005**, *24*, 6301−6309.
(84) de Frémont, P.; Scott, N. M.; Stevens, E. D.; Nolan, S. P. *Organometallics* **2005**, *24*, 2411−2418.
(85) Frisch, M. J.; Trucks, G. W.; Schlegel, H. B.; Scuseria, G. E.; Robb, M. A.; Cheeseman, J. R.; Scalmani, G.; Barone, V.; Mennucci, B.; Petersson, G. A.; Nakatsuji, H.; Caricato, M.; Li, X.; Hratchian, H. P.; Izmaylov, A. F.; Bloino, J.; Zheng, G.; Sonnenberg, J. L.; Hada, M.; Ehara, M.; Toyota, K.; Fukuda, R.; Hasegawa, J.; Ishida, M.; Nakajima, T.; Honda, Y.; Kitao, O.; Nakai, H.; Vreven, T.; Montgomery, J. A., Jr., Peralta, J. E.; Ogliaro, F.; Bearpark, M.; Heyd, J. J.; Brothers, E.; Kudin, K. N.; Staroverov, V. N.; Keith, T.; Kobayashi, R.; Normand, J.; Raghavachari, K.; Rendell, A.; Burant, J. C.; Iyengar, S. S.; Tomasi, J.; Cossi, M.; Rega, N.; Millam, J. M.; Klene, M.; Knox, J. E.; Cross, J. B.; Bakken, V.; Adamo, C.; Jaramillo, J.; Gomperts, R.; Stratmann, R. E.; Yazyev, O.; Austin, A. J.; Cammi, R.; Pomelli, C.; Ochterski, J. W.; Martin, R. L.; Morokuma, K.; Zakrzewski, V. G.; Voth, G. A.; Salvador, P.; Dannenberg, J. J.; Dapprich, S.; Daniels, A. D.; Farkas, O.; Foresman, J. B.; Ortiz, J. V.; Cioslowski, J.;, Fox, D. J. *Gaussian 09*, Revision B.01; Gaussian, Inc.: Wallingford, CT, 2010.
(86) Becke, A. D. *Phys. Rev. A: At., Mol., Opt. Phys.* **1988**, *38*, 3098.
(87) Perdew, J. *Phys. Rev. B: Condens. Matter Mater. Phys.* **1986**, *33*, 8822−8824.
(88) Hay, P. J.; Wadt, W. R. *J. Chem. Phys.* **1985**, *82*, 299−13.
(89) Roy, L. E.; Hay, P. J.; Martin, R. L. *J. Chem. Theory Comput.* **2008**, *4*, 1029−1031.
(90) Ehlers, A. W.; Böhme, M.; Dapprich, S.; Gobbi, A.; Höllwarth, A.; Jonas, V.; Köhler, K. F.; Stegmann, R.; Veldkamp, A.; Frenking, G. *Chem. Phys. Lett.* **1993**, *208*, 111−114.
(91) Hay, P. J.; Wadt, W. R. *J. Chem. Phys.* **1985**, *82*, 270.
(92) Wadt, W. R.; Hay, P. J. *J. Chem. Phys.* **1985**, *82*, 284−16.
(93) Tomasi, J.; Mennucci, B.; Cammi, R. *Chem. Rev.* **2005**, *105*, 2999−3094.
(94) Glendening, E. D.; Reed, A. E.; Carpenter, J. E.; Weinhold, F. *NBO* Version 3.1.



DOI: 10.1021/acs.organomet.5b00476
*Organometallics* 2015, 34, 3857−3864